Neurobiology of Disease 130 (2019) 104498

Contents lists available at ScienceDirect

Neurobiology of Disease

journal homepage: www.elsevier.com/locate/ynbdi

Cyclophillin A deficiency accelerates RML-induced prion disease

Ihssane Bouybayoune[a,1,2], Liliana Comerio[a,2], Laura Pasetto[b], Ilaria Bertani[a], Valentina Bonetto[b], Roberto Chiesa[a,*]

[a] Department of Neuroscience, Istituto di Ricerche Farmacologiche Mario Negri IRCCS, 20156 Milano, Italy
[b] Department of Biochemistry and Molecular Pharmacology, Istituto di Ricerche Farmacologiche Mario Negri IRCCS, 20156 Milano, Italy

ARTICLE INFO

Keywords:
Protein misfolding
Prion protein
PrP
Scrapie
PPIA
Microglia
Neuroinflamation

ABSTRACT

Prion diseases typically involve brain deposition of abnormally folded prion protein, which is associated with activated glia and increased cytokine production. Cyclophilin A (CypA) is a ubiquitous protein with peptidyl prolyl *cis-trans* isomerase activity, which regulates protein folding, and can be secreted by cells in response to inflammatory stimuli. On the basis of *in vitro* studies, CypA was proposed to mediate glial activation during prion infection. To investigate the role of CypA *in vivo*, we inoculated CypA$^{+/+}$, CypA$^{+/-}$ and CypA$^{-/-}$ mice with the RML prion strain, and recorded the time to onset of neurological signs and to terminal disease, and the astrocyte and microglia response at presymptomatic and symptomatic stages. Time to onset of disease and survival were significantly shorter in CypA-deficient mice than CypA-expressing controls. CypA-deficient mice had significantly greater microglial activation in the presymptomatic stage, and analysis of anti- and pro-inflammatory microglial markers indicated a shift towards a pro-inflammatory phenotype. There was no difference in astrocyte activation. This suggests that CypA contributes to dampening the pro-inflammatory microglial response during the early stage of RML-induced prion disease.

1. Introduction

Prion diseases, including scrapie of sheep and goat, chronic wasting disease of deer and elk, bovine spongiform encephalopathy and its human counterpart, variant Creutzfeld-Jakob disease (vCJD), are fatal infections of the central nervous system (CNS). The infectious agent (prion) is PrP^{Sc}, an aggregated and partially protease-resistant isoform of the cellular prion protein (PrP^{C}), which replicates by inducing misfolding and aggregation of host-encoded PrP^{C} (Colby and Prusiner, 2011).

Accumulation of PrP^{Sc} in the CNS is associated with activation of microglia, proliferation and hypertrophy of astrocytes, spongiform change (vacuolation of the neuropil in the gray matter), synaptic degeneration and neuronal loss (Sikorska et al., 2012). In scrapie-infected mice, gliosis occurs at an early stage of the disease and in areas of proteinase-K (PK)-resistant PrP^{Sc} deposition, and precedes spongiosis and neuronal loss (Carroll et al., 2016).

Glial activation during prion infection is accompanied by upregulation of neuroinflammatory genes and cytokine production (Carroll et al., 2016). This response may have both beneficial and detrimental effects (Aguzzi and Zhu, 2017; Carroll and Chesebro, 2019; Hickman et al., 2018). Phagocytic microglia may engulf PrP^{Sc} aggregates, helping to reduce the prion load (Carroll et al., 2018; Zhu et al., 2016); however, the increase in cytokine production that accompanies glial activation may contribute to neuronal dysfunction and degeneration. Proinflammatory cytokines such as tumor necrosis factor α (TNFα) and interleukin-1β (IL-1β) are elevated in vCJD and in experimental scrapie (Kordek et al., 1996; Sharief et al., 1999), and prion-infected mice with amplified expression of IL-1β have accelerated disease progression and exacerbated neuropathology (Cunningham et al., 2005; Field et al., 2010). In contrast, the onset and progression of disease are delayed in IL-1 receptor I-deficient mice (Schultz et al., 2004; Tamguney et al., 2008), and the IL-1 receptor antagonist anakinra rescues the neurophysiological deficits and lowers the threshold for seizures in a mouse model of CJD in which IL-1β is produced by reactive astrocytes (Bertani et al., 2017).

The mechanisms responsible for glial activation in prion diseases are not clear. Tribouillard-Tanvier and colleagues found that exposure of cultured microglia or astroglia to scrapie-infected brain homogenates induced the release of several cytokines (Tribouillard-Tanvier et al.,

* Corresponding author.
E-mail address: roberto.chiesa@marionegri.it (R. Chiesa).
[1] Present address: School of Cancer & Pharmaceutical Sciences, King's College London, SE1 9RT, London, UK
[2] I.Bo. and L.C. contributed equally to this work

https://doi.org/10.1016/j.nbd.2019.104498
Received 2 April 2019; Received in revised form 14 May 2019; Accepted 5 June 2019
Available online 08 June 2019
0969-9961/

2009). They used a brain fractionation approach and mass spectrometry to identify the stimulatory factor(s), and found that the active scrapie brain fraction contained several low-molecular-weight proteins that stimulate cytokine release, including cyclophilin A (CypA) (Tribouillard-Tanvier et al., 2012). The cytokine stimulating effect of the active scrapie brain fraction was reduced by co-incubation with an anti-CypA antibody or cyclosporin A (CsA), a CypA inhibitor (Tribouillard-Tanvier et al., 2012). Moreover, purified fragments of recombinant CypA had glial stimulatory effects comparable to those triggered by the active scrapie brain fraction (Tribouillard-Tanvier et al., 2012). Thus CypA was proposed as a primary mediator of gliosis in prion infection.

CypA, also known as peptidyl prolyl cis−/trans isomerase A (PPIA), is a ubiquitous protein highly expressed in the CNS, belonging to the immunophilin family. Its PPIase activity regulates protein folding and trafficking. Although CypA was initially believed to have mainly intracellular functions, recent studies have shown that it can be secreted by cells in response to inflammatory stimuli (Dawar et al., 2017). There is also evidence supporting a critical function of CypA in neurodegenerative disorders involving accumulation of aggregated proteins, such as Alzheimer's disease (Bell et al., 2012) and amyotrophic lateral sclerosis (ALS) (Lauranzano et al., 2015; Pasetto et al., 2017). Given its proposed role as a mediator of glial activation in prion diseases, and its emerging involvement in protein misfolding diseases of the CNS, we investigated the effects of genetic ablation of CypA on the natural history of disease in prion-infected mice.

2. Results

2.1. CypA-deficient mice have a shorter incubation time and faster disease progression

Groups of $CypA^{+/+}$, $CypA^{+/-}$ and $CypA^{-/-}$ littermate mice were inoculated intracerebrally with the mouse-adapted scrapie strain RML. Some animals in each group were culled for histological and biochemical analyses at 70 and 110 days post-inoculation (d.p.i.), corresponding respectively to early and late presymptomatic stages of the disease in RML-inoculated wild-type mice. The remaining mice were monitored for the appearance of clinical signs of scrapie and killed when they reached the terminal stage of disease, as described in the Material and Methods. The incubation period was slightly but significantly shorter in $CypA^{-/-}$ than $CypA^{+/-}$ and $CypA^{+/+}$ mice (Fig. 1A and Table 1). There was a CypA gene-dosage effect, with time to onset of disease in $CypA^{+/-}$ and $CypA^{-/-}$ mice 3 and 6% shorter than in $CypA^{+/+}$ mice (Table 1). Time to end-stage disease was also significantly reduced in a gene dose-dependent manner, with $CypA^{+/-}$ and $CypA^{-/-}$ surviving 3.5% and 7% less than $CypA^{+/+}$ mice (Fig. 1B and Table 1).

2.2. CypA deficiency does not influence PrP^{Sc} accumulation in RML-infected mice

To test whether CypA deficiency altered the progressive accumulation of PrP^{Sc}, we assayed protease-resistant and detergent-insoluble PrP at 70, 110 d.p.i. and at the end-stage of disease. Brains were homogenized in a Triton-X100/deoxycholate buffer, incubated with or without PK, and analyzed by Western blot. Analysis of the undigested samples with an anti-CypA antibody confirmed the absence of the CypA protein in $CypA^{-/-}$ mice and showed lower CypA levels in $CypA^{+/-}$ mice (Fig. 2, upper panel). PK-resistant PrP was barely detectable at 70 d.p.i., but was clearly seen at 110 d.p.i. and at end-stage disease. There were no differences in the amount and/or glycosylation pattern of the PK-resistant PrP fragments between mice of the different CypA genotypes (Fig. 2, lower panel). Immunohistochemistry of PrP in brain sections found no differences in the amount and distribution of protease-resistant PrP between $CypA^{+/+}$, $CypA^{+/-}$ and $CypA^{-/-}$ mice

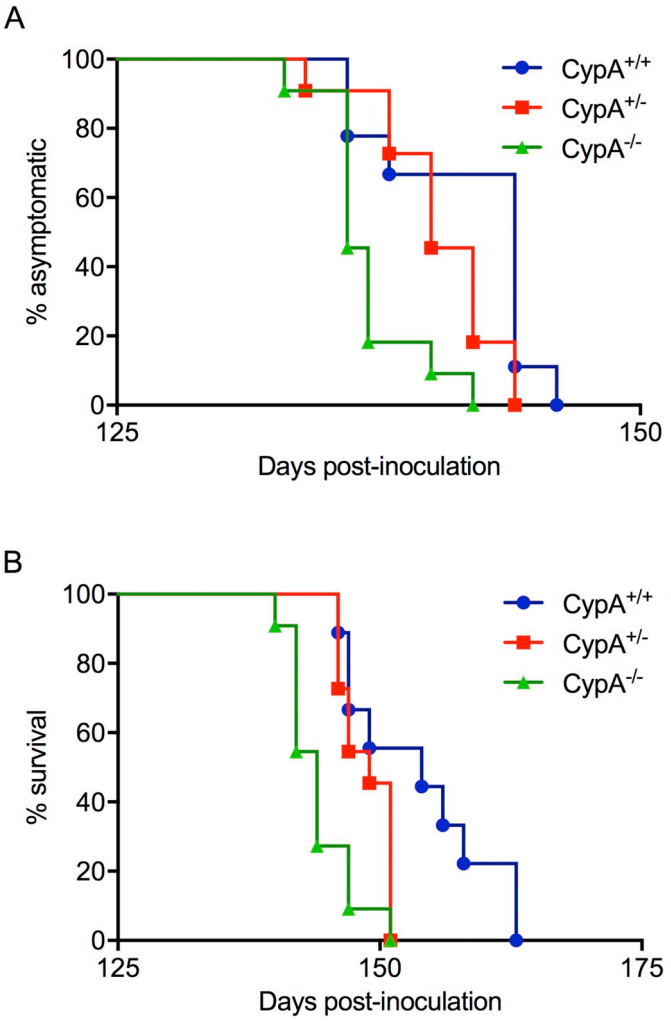

Fig. 1. Incubation and survival times are shorter in RML-inoculated CypA-deficient mice. Kaplan-Meier plots showing time to onset of disease (A) and time to terminal illness (B) of 9 $CypA^{+/+}$ (●), 11 $CypA^{+/-}$ (■) and 11 $CypA^{-/-}$ (▲) mice inoculated with a 10^{-3} dilution of RML scrapie-infected brain homogenate. (A) Time to onset of disease was 3% and 6% shorter than in $CypA^{+/-}$ and $CypA^{+/+}$ mice ($p < .05$; Log-rank Test). (B) Time to death was significantly reduced, with $CypA^{-/-}$ mice surviving 3.5% and 7% less than $CypA^{+/-}$ and $CypA^{+/+}$ mice ($p < .05$ and $p < .001$; Log-rank Test).

(not shown).

To assay detergent-insoluble PrP, brain extracts were centrifuged at 18,000 *x g* for 2 min, the supernatant was collected and ultracentrifuged at 186,000 *x g* for 45 min. The proteins in the first and second pellets (P_0 and P), and in the final supernatant (S) were analyzed by Western blot, and the PrP in the different fractions was quantified by densitometry and expressed as percentages of the amount of PrP in all the fractions. Most PrP in brain extracts from uninfected $CypA^{+/+}$, $CypA^{+/-}$ and $CypA^{-/-}$ mice was recovered in the S fractions (Fig. 3A). In RML-infected mice culled at 70 d.p.i., 30–40% of PrP was found in the insoluble P and P_0 fractions (Fig. 3B). The insoluble fraction increased further with disease progression, with almost all PrP recovered in the P_0 fractions at 110 d.p.i. and at the end-stage of disease (Fig. 3C and D). There was no significant difference in the distribution of PrP in the different fractions between mice of the different genotypes at any of the disease stages.

2.3. CypA deficiency does not affect RML-induced neurodegeneration

Hematoxylin and eosin staining of brain sections showed similar

Table 1
Onset of disease and survival of RML-infected CypA$^{+/+}$, CypA$^{+/-}$ and CypA$^{-/-}$ mice.

CypA genotype	Median onset (days)	Change in median onset (days; percentage)	Hazard ratio (95% confidence interval)	p value
+/+	144			
+/−	140	4 (2.9%)	0.36 (0.11–1.18)	ns
−/−	136	8 (5.8%)	0.14 (0.04–0.48)	< 0.01 *vs.* +/+ and +/−
CypA genotype	Median survival (days)	Change in median survival (days; percentage)	Hazard ratio (95% confidence interval)	p value
+/+	154			
+/−	149	5 (3.35%)	0.30 (0.09–0.98)	< 0.05 *vs.* +/+
−/−	144	10 (6.9%)	0.13 (0.04–0.43)	< 0.001 *vs.* +/+ < 0.01 *vs.* +/−

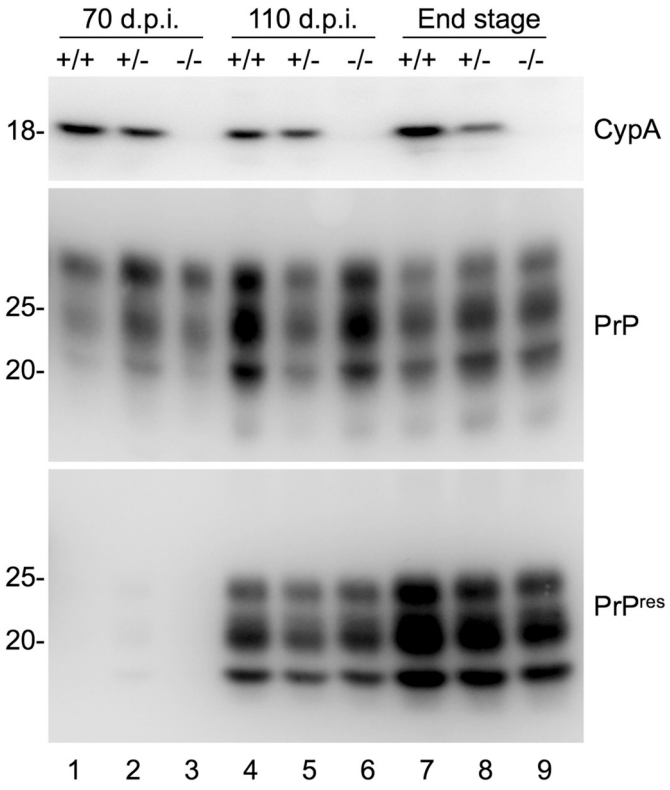

Fig. 2. CypA deficiency does not influence PK-resistant PrP accumulation in RML-inoculated mice. Brain extracts of CypA$^{+/+}$, CypA$^{+/-}$ and CypA$^{-/-}$ mice culled at 70 or 110 days post-inoculation (d.p.i.), or at the end stage of disease, were incubated with 0 (top and middle panels) or 5 μg/mL of PK for 30 min at 37 °C (lower panel), and analyzed by Western blot using an anti-CypA antibody (top panel) or anti-PrP antibody 6H4 (middle and lower panels). Very faint PK-resistant PrP bands are detectable at 70 d.p.i. The amounts and glycosylation patterns of the PK-resistant PrP fragments were similar in CypA$^{+/+}$, CypA$^{+/-}$ and CypA$^{-/-}$ mice at 110 d.p.i. and at the end stage of disease. The experiment shown is representative of three replicates.

spongiform changes in CypA$^{+/+}$, CypA$^{+/-}$ and CypA$^{-/-}$ mice (Fig. 4A). The number of neurons in the CA1 area of the hippocampus, which undergo massive degeneration in the RML model (Moreno et al., 2013), was similar in terminally ill mice of the different CypA genotypes (CypA$^{+/+}$ = 229 ± 21; CypA$^{+/-}$ = 355 ± 43; CypA$^{-/-}$ = 324 ± 30; mean ± SEM of 20–36 sections from two animals per group; $F_{2,86} = 2.617$; $p = .0788$ by one-way ANOVA). Western blot of total brain homogenates found reduced levels of the synaptic marker synaptophysin in RML-infected mice at the terminal stage of disease, but no significant differences between CypA-expressing and CypA-deficient mice (Fig. 4B and C). Thus, the hastened disease course in CypA-deficient mice was not associated with more neurodegeneration.

2.4. CypA-deficient mice have increased microglial activation at an early disease stage

Immunohistochemical analysis of brain sections with an anti-glial fibrillary acidic protein (GFAP) antibody detected similar astrocytosis in mice of the different CypA genotypes at pre-symptomatic and end stages (Fig. 5A). Consistent with this, Western blot analysis of brain homogenates found increased levels of GFAP in both CypA-expressing and -deficient mice (Fig. 5B and C).

Analysis of microglia with an anti-ionized calcium-binding adapter molecule 1 (IBA1) antibody showed marked microgliosis in CypA-deficient mice at 70 d.p.i., with the IBA1-positive area fraction significantly larger in CypA$^{-/-}$ than CypA$^{+/-}$ and CypA$^{+/+}$ animals (Fig. 6A panels i-iii, and 6B). At the end-stage of disease microglia were further activated, but to a similar extent in mice of the different CypA genotypes (Fig. 6A panels iv-vi, and 6C). Supporting earlier microglial activation in CypA-deficient mice, Western blot analysis of brain homogenates showed large amounts of IBA1 in CypA$^{-/-}$ mice at 70 d.p.i., which equaled those found in CypA$^{+/+}$ and CypA$^{-/-}$ mice at the end-stage of disease (Fig. 6D and E).

To address the functional commitment of activated microglia, we measured M2-like (heparin-binding lectin Ym1) and M1-like (TNFα) markers. The levels of Ym1 were significantly lower in CypA$^{-/-}$ than in CypA$^{+/+}$ mice at 70 d.p.i., whereas TNFα levels were comparable (Fig. 7). At the end stage, the levels of both proteins were significantly higher in CypA$^{-/-}$ than CypA$^{+/+}$ mice (Fig. 7). This suggests a shift towards a pro-inflammatory microglia phenotype in mice lacking CypA.

3. Discussion

Genetic CypA ablation shortened the incubation time and survival in RML-infected mice, with earlier microglia activation and changes in microglial markers consistent with a shift towards a proinflammatory phenotype. These results indicate that CypA may contribute to attenuating proinflammatory microglial activation during the early phase of prion infection, and support the emerging immunomodulatory role of CypA in neurodegenerative diseases of the CNS.

We found that CypA deletion accelerated RML-induced disease without any significant effect on the degree of neurodegeneration, as shown by analysis of synaptophysin levels and direct count of hippocampal CA1 neurons, which are particularly vulnerable to the RML strain. There was also no obvious difference in spongiosis between CypA-expressing and -deficient mice. Since CypA$^{+/-}$ and CypA$^{-/-}$ mice have no supernumerary neurons in the hippocampus which could have masked enhanced neurodegeneration (data not shown), other factors may have contributed to aggravate the clinical outcome of scrapie in these mice.

CypA is mainly found in the cytoplasm, but can also be released in the extracellular space. It has PPIase activity that induces the *cis-trans* isomerization of peptidyl-prolyl bonds. This activity is important in cytosolic protein folding and assembly, but can also affect the structure

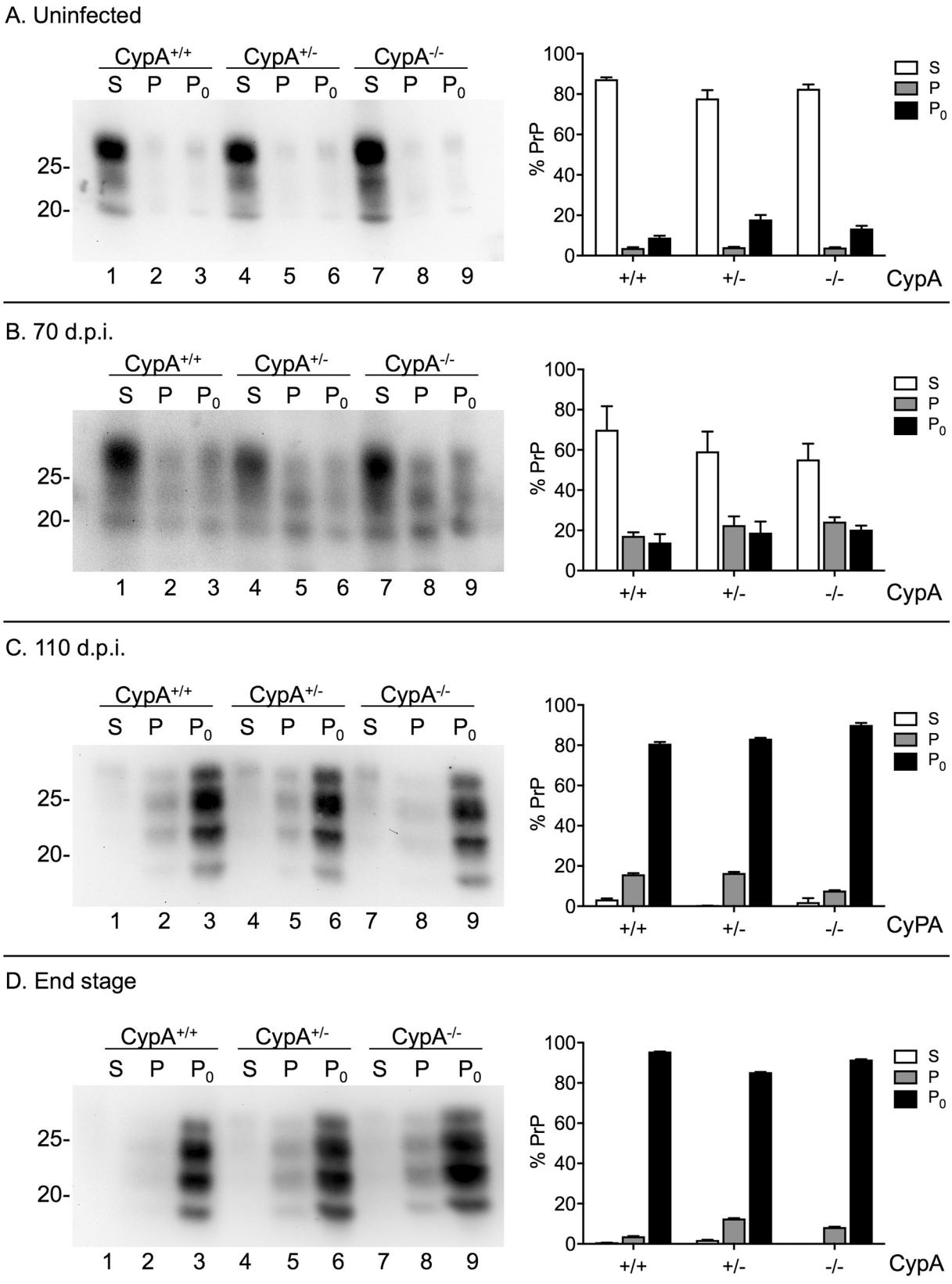

Fig. 3. CypA deficiency does not influence the amount of detergent-insoluble PrP. Mouse brain extracts were centrifuged at 18,000 x *g* for 2 min. The pellet (P_0) was recovered and the supernatant was ultracentrifuged at 186,000 x *g* for 45 min. PrP in each fraction [final supernatant (S), first (P_0) and the second pellet (P)] was analyzed by Western blot using the monoclonal antibody 12B2, quantified by densitometry and expressed as a percentage of the total amount of PrP. No significant differences in the distribution of PrP in the S, P and P_0 fractions were found between CypA $^{-/-}$, CypA $^{+/-}$ and CypA $^{+/+}$ mice, either uninfected (A), or RML-infected at 70 d.p.i. (B), 110 (C) d.p.i. or at the end-stage of disease (D). Data are the mean ± SD of 3–5 replicate experiments using brains from 2 to 3 mice of each genotype.

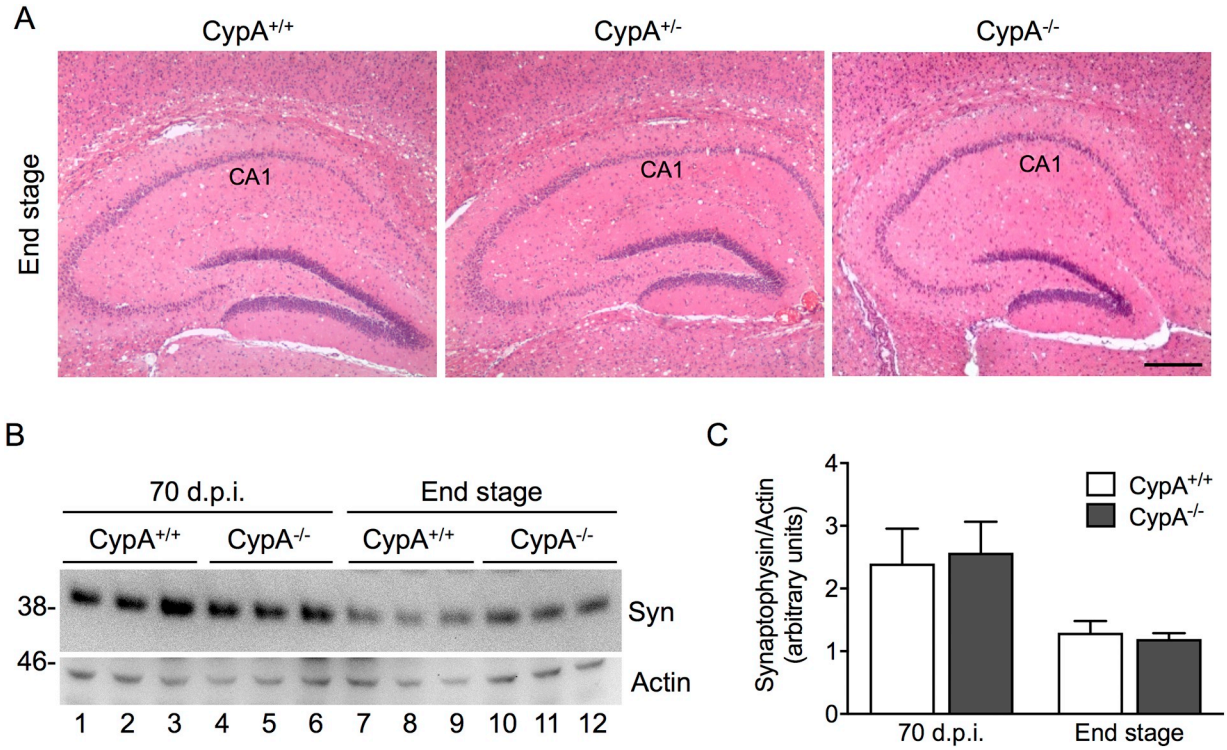

Fig. 4. CypA$^{+/+}$, CypA$^{+/-}$ and CypA$^{-/-}$ mice show similar neurodegenerative changes. (A) Representative images showing hematoxylin and eosin staining of the hippocampus of CypA$^{+/+}$, CypA$^{+/-}$ and CypA$^{-/-}$ mice at the end stage of disease. Scale bar: 250 µm. (B) Brain homogenates from CypA$^{+/+}$ and CypA$^{-/-}$ mice were analyzed by Western blot with anti-synaptophysin (Syn) and anti-actin antibodies. Synaptophysin levels were quantified by densitometry, normalized for the level of actin and expressed as percentages of the level in CypA$^{+/+}$ mice at 70 d.p.i. Data are the mean ± SEM of two independent experiments using brains from three mice of each genotype. $F_{3,15} = 4.897$; $p = .0144$ by two-way ANOVA.

and activity of cell surface proteins, as in the case of CD147 and the prolactin receptor (Yurchenko et al., 2002; Syed et al., 2003). PrP^{C} is rich in proline residues, specially in the N-terminal octapeptide repeat region, which makes it a potential substrate of CypA PPIase. Peptidyl-prolyl isomerization may affect the conformation of cell surface PrP^{C} and its propensity to interact with PrP^{Sc} and/or undergo PrP^{Sc}-induced conformational conversion. However, we found no differences in the amounts of protease-resistant and detergent-insoluble PrP between CypA-expressing and -deficient mice, indicating that the propensity to PrP^{Sc} conversion was not affected. In line with this, genetic ablation of peptidyl-prolyl-isomerase 1 also had no effect on PrP^{Sc} accumulation in RML-infected mice, and did not influence PrP^{Sc} replication by protein misfolding cyclic amplification (Legname et al., 2018).

Inhibition of the cyclophilin family of PPIases by CsA induced the formation of potentially neurotoxic cytosolic PrP species in cultured cells (Cohen and Taraboulos, 2003), raising the possibility that an increased propensity to cytosolic PrP formation may have contributed to aggravating RML-induced disease in CypA$^{+/-}$ and CypA$^{-/-}$ mice. However, inhibition of endoplasmic reticulum-resident CypB, rather than cytosolic CypA, appears to be primarily responsible for the generation of cytosolic PrP in CsA-treated cells. Consistent with this, we found no biochemical evidence of increased cytosolic PrP in RML-infected CypA-deficient mice. In addition, the neurotoxicity of cytosolic PrP has been questioned, with a number of studies showing a neuroprotective role of this topological isoform (Roucou et al., 2003; Restelli et al., 2010; Fioriti et al., 2005; Quaglio et al., 2011).

Genetic CypA depletion brought forward the onset of disease and reduced the life span in the SOD1^{G93A} mouse model of ALS, without exacerbating motor neuron degeneration (Lauranzano et al., 2015). The amount of insoluble TDP-43, a RNA binding protein whose assembly in heterogeneous nuclear ribonucleoprotein (hnRNP) complexes requires CypA, was increased in CypA$^{-/-}$ mice and quite likely contributed to aggravating the neurological illness in the SOD1^{G93A}/CypA$^{-/-}$ model. This suggests that TDP-43 pathology may contribute to hastening the disease also in RML-infected CypA-deficient mice.

Glia are activated during the early stages of prion infection before neuronal loss, spongiform change, and the onset of clinical signs (Williams et al., 1997). Genetic or pharmacological microglial depletion enhanced PrP^{Sc} deposition and neurodegeneration in prion-infected organotypic cerebellar cultures, and raised brain PrP^{Sc} levels and hastened disease progression in scrapie-infected mice (Carroll et al., 2018; Zhu et al., 2016; Falsig et al., 2008). These detrimental effects were explained by the ability of microglia to phagocyte and degrade PrP^{Sc}, bringing to light a neuroprotective role of microglia in prion infection. We found increased microglia activation in CypA-deficient mice at 70 d.p.i., but the amounts of PK-resistant and detergent-insoluble PrP were not reduced at this or later disease stages, suggesting that phagocytic activity was not boosted.

However, microglia can take on activation profiles with detrimental effects, and there is evidence that much of the pro-inflammatory response in experimental models of prion infection is attributable to this cell type (Vincenti et al., 2015). At 70 d.p.i., CypA-deficient mice had lower brain levels of Ym1 than CypA-expressing animals, but similar TNFα levels, suggesting a shift towards a pro-inflammatory microglial polarization. At the end stage, CypA$^{-/-}$ mice had higher TNFα levels. Pro-inflammatory cytokines such as TNFα and IL-1β can exacerbate neurological dysfunction in neurodegenerative conditions such as prion diseases through modifications in neuronal network excitability (Bertani et al., 2017; Vezzani and Viviani, 2015). This may account for the acceleration of scrapie disease in CypA-deficient mice.

RML-induced astrocytosis was not enhanced in CypA-deficient mice at any disease stage, as indicated by GFAP immunostaining and Western blot analysis, suggesting no effect on this glial cell type. However, it is becoming clear that, like microglia, astrocytes can

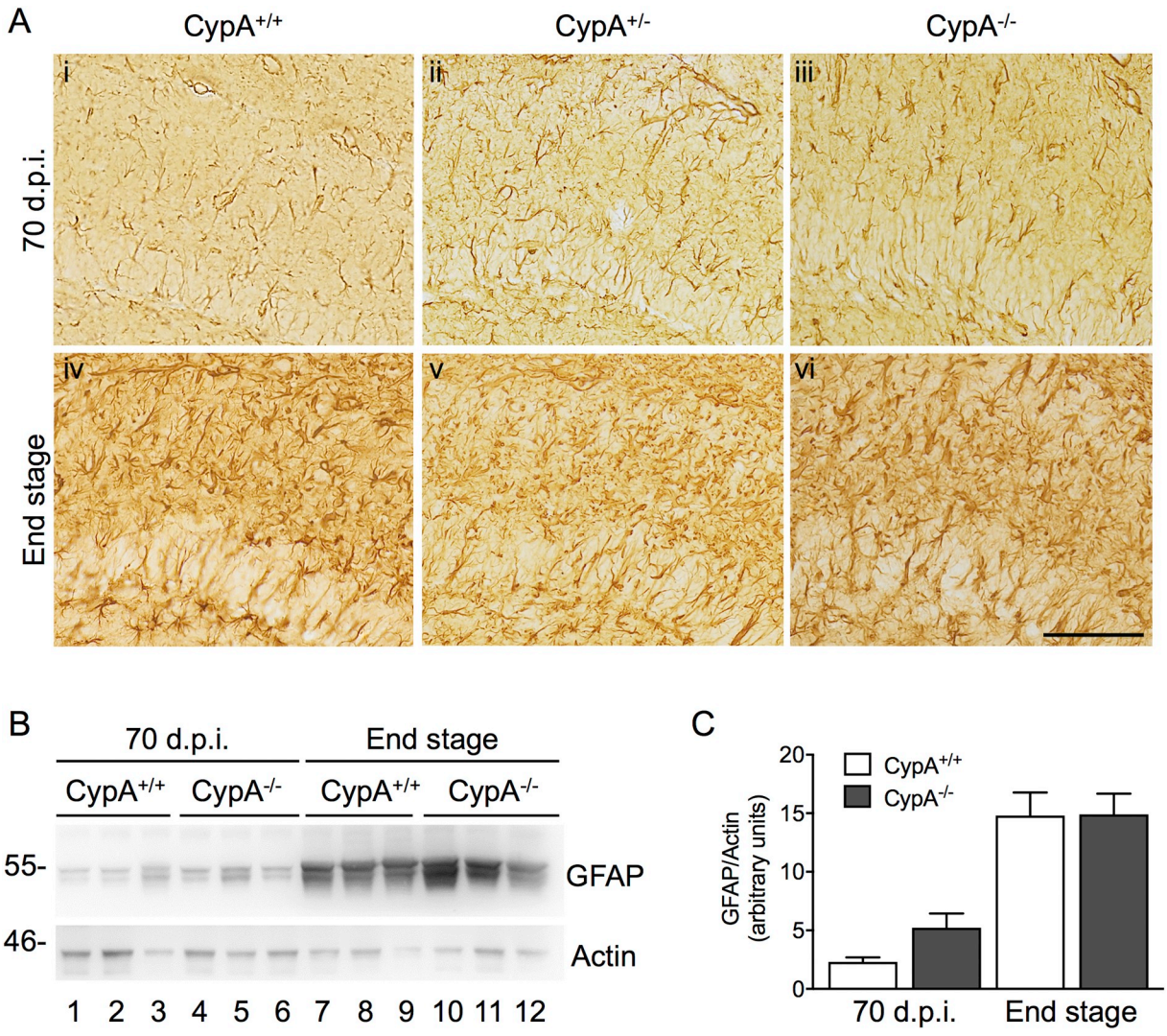

Fig. 5. CypA$^{+/+}$, CypA$^{+/-}$ and CypA$^{-/-}$ mice show similar astrocytosis. (A) Representative images showing immunohistochemical detection of astrocytes in the hippocampus of RML-infected CypA$^{+/+}$, CypA$^{+/-}$ and CypA$^{-/-}$ mice using a monoclonal antibody anti-GFAP. No differences in degree of astrocytosis are seen at 70 d.p.i. (i-iii) or at the end stage (iv-vi) between mice of the three CypA genotypes. Scale bar: 50 µm. (B) Brain homogenates from CypA$^{+/+}$ and CypA$^{-/-}$ mice were analyzed by Western blot with anti-GFAP and anti-actin antibodies. GFAP levels were quantified by densitometry and normalized for the level of actin. Data are the mean ± SEM of two independent experiments using brains from three mice of each genotype. $F_{3,18} = 18.88$; $p < .0001$ by two-way ANOVA.

assume different functional states, including the neurotoxic A1 phenotype (Liddelow and Barres, 2017; Liddelow et al., 2017). It will be interesting to see whether a molecular A1 signature emerges during RML infection and if CypA deletion promotes acquisition of this noxious cell phenotype.

In summary, our *in vivo* analysis of the consequences of CypA deficiency in prion infection indicates a protective immunomodulatory role of this protein which contrasts with its proposed role as a mediator of prion-induced neuroinflammation suggested *in vitro* (Tribouillard-Tanvier et al., 2012). However, neuroinflammatory CypA activity *in vitro* was attributed to truncated fragments of CypA *via* CD147 binding and not to the full-length protein. In fact, specific inhibition of extracellular CypA isoforms was neuroprotective in a SOD1^{G93A} ALS mouse model by reducing CD147-activated neuroinflammation, while genetic CypA ablation was not (Lauranzano et al., 2015; Pasetto et al., 2017). It would be interesting to use cell-impermeable CsA derivatives (Malesević et al., 2010) in RML-infected mice to specifically assess the contribution of extracellular CypA in disease pathogenesis.

4. Materials and methods

4.1. Animal models

Procedures involving animals were conducted in conformity with the institutional guidelines at the Istituto di Ricerche Farmacologiche Mario Negri IRCCS, in compliance with national (D.lgs 26/2014; Authorization n. 19/2008-A issued March 6, 2008 by Ministry of Health) and international laws and policies (EEC Council Directive 2010/63/UE; the NIH Guide for the Care and Use of Laboratory Animals, 2011 edition). They were reviewed and approved by the Mario Negri Institute Animal Care and Use Committee, which includes *ad hoc* members for ethical issues, and by the Italian Ministry of Health (Decreto no. 370/2016-PR and 386/2015-PR). Animal facilities meet international standards and are regularly checked by a certified veterinarian who is responsible for health monitoring, animal welfare supervision, experimental protocols and review of procedures.

CypA$^{-/-}$ (*PPIA*$^{-/-}$) mice (strain 129S6/SvEvTac Ppiatm1Lubn/

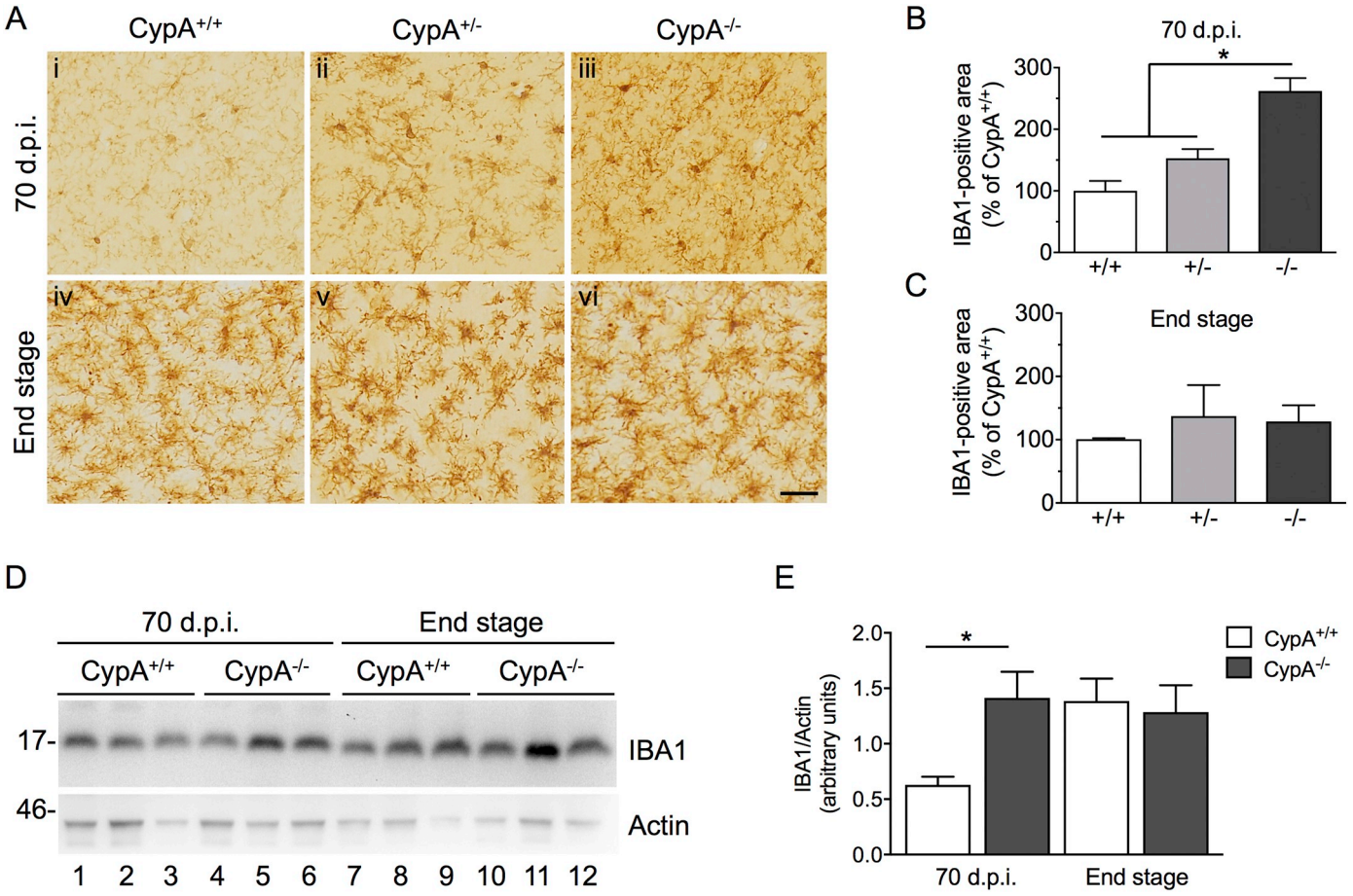

Fig. 6. Increased microglial activation in CypA$^{-/-}$ mice at an early stage of disease. (A) Representative images of immunohistochemical detection of microglia in the hippocampus using a polyclonal antibody anti-IBA1. CypA$^{-/-}$ mice at 70 d.p.i. show marked microglia activation compared to CypA$^{+/+}$ and CypA$^{+/-}$ (panels i-iii). No differences are seen at the end stage of disease (panels iv-vi). Scale bar: 25 µm. (B) Quantification of the IBA1-positive area in the hippocampus of RML-inoculated mice at 70 d.p.i. Data are the mean ± SEM of 8–10 sections from two mice of each genotype. $F_{2,3} = 19.92$; $p = .0185$ by one-way ANOVA; *p < .05 Tukey's post-hoc test. (C) Quantification of the IBA1-positive area in the hippocampus of end-stage diseased animals. Data are the mean ± SEM of 23–28 sections from four mice of each genotype. $F_{2,9} = 0.3582$; $p = .7085$ by one-way ANOVA. (D) Brain homogenates from CypA$^{+/+}$ and CypA$^{-/-}$ mice were analyzed by Western blot with anti-IBA1 and anti-actin antibodies. (E) IBA1 levels were quantified by densitometry and normalized for the level of actin. Data are the mean ± SEM of two independent experiments using brains from three mice of each genotype. $F_{3,18} = 4.994$; $p = .0108$ by two-way ANOVA; *p < .05 Tukey's post-hoc test.

Ppiatm1Lbn; stock no. 005320) (Colgan et al., 2004) were obtained from The Jackson Laboratory and maintained on a 129S6/SvEvTac background. They were genotyped by standard PCR as recommended by The Jackson Laboratory.

4.2. Prion transmission

One percent (*w/v*) of RML scrapie-infected brain homogenate was prepared in phosphate-buffered saline (PBS) and cleared by centrifugation at 900 ×*g* for 5 min; 25 µL of the cleared homogenate was injected intracerebrally into the right parietal lobe of CypA$^{+/+}$, CypA$^{+/-}$ and CypA$^{-/-}$ mice using a 25-gauge needle. Mice were observed weekly for signs of neurological dysfunction according to a set of objective criteria (Bouybayoune et al., 2015). Onset of disease was scored as the time at which at least two neurological signs were observed, out of foot-clasp reflex, kyphosis, unbalanced body posture, difficulty walking on a horizontal metal grid and remaining on a vertical grid for at least 30 s. Terminal disease was scored when mice became unable to right themselves from a supine position in < 60 s, to walk on a horizontal metal grid, and/or had cumulative weight loss equivalent to 20% of their body mass since the onset of disease.

4.3. Biochemical analyses

Tissue homogenates were prepared in PBS using a glass/Teflon tissue homogenizer. Detergent insolubility and proteinase-K resistance were assayed as described (Chiesa et al., 1998). Western blots were developed with: mouse monoclonal anti-PrP antibodies 12B2 (Central Veterinary Institute, Wageningen, NL, 1:5000) or 6H4 (Prionics, 1:5000), anti-cyclophilin A (Millipore #07-313, 1:500), mouse monoclonal anti-glial fibrillary acidic protein (GFAP) antibody (Abcam ab9484, 1:2000), rabbit polyclonal anti-ionized calcium binding adapter molecule 1 (Iba1) (Wako Reagent, 1:1000), anti-synaptophisin (SYSY 101–002, 1:5000), anti-TNFα (abcam ab34674, 1:500) and anti-Ym1 (STEMCELL #60130, 1:1000).

4.4. Histology

Brains were fixed in Alcolin (Diapath), dehydrated in graded ethanol solutions, cleared in xylene, and embedded in paraffin. Serial sections (8 µm thick) were cut and stained with hematoxylin and eosin.

For GFAP and Iba1 immunohistochemistry, mice were deeply anesthetized and perfused through the ascending aorta with phosphate

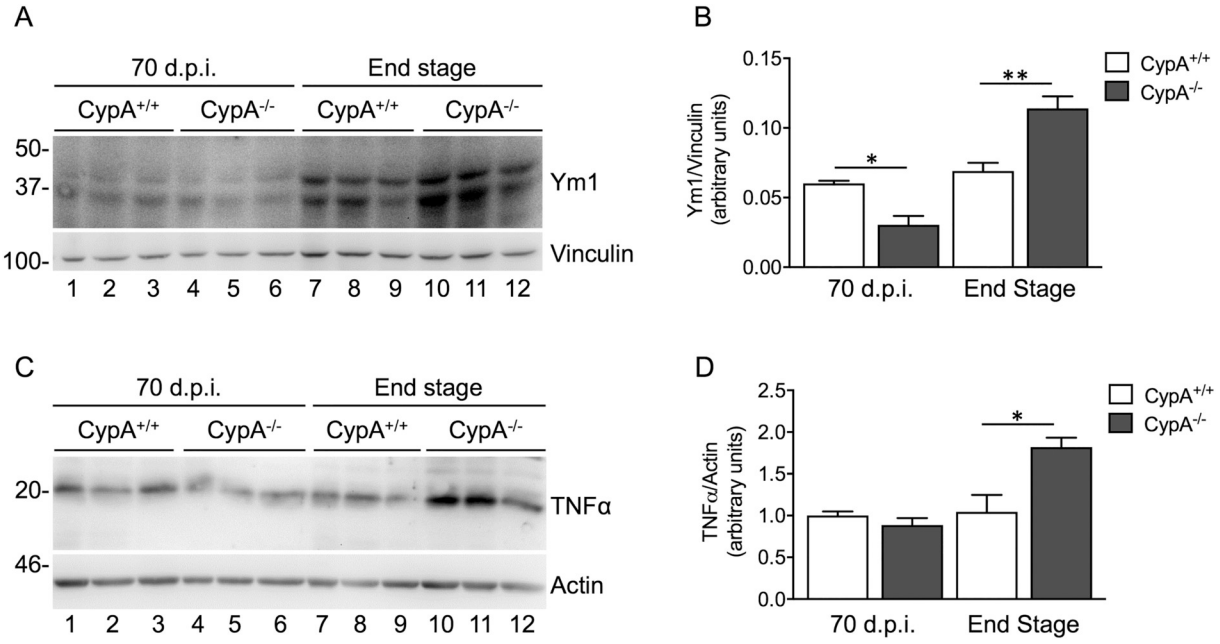

Fig. 7. Ym1 and TNFα levels in the brain of RML-infected CypA$^{+/+}$ and CypA$^{-/-}$ mice. (A) Brain homogenates from CypA$^{+/+}$ and CypA$^{-/-}$ mice were analyzed by Western blot with anti-Ym1 and anti-vinculin antibodies. Ym1 levels were quantified by densitometry and normalized for the level of vinculin. Data are the mean ± SEM of three mice of each genotype. $F_{3,6} = 32.91$; $p = .0004$ by two-way ANOVA; *p < .05, ** p < .001 Tukey's post-hoc test. (B) The brain homogenates used in A were analyzed by Western blot with anti-TNFα and anti-actin antibodies. TNFα levels were quantified by densitometry and normalized for the level of actin. Data are the mean ± SEM of three mice of each genotype. $F_{3,6} = 9.273$; $p = .0114$ by two-way ANOVA; *p < .05 Tukey's post-hoc test.

buffered saline (PBS, 0.05 M; pH 7.4) followed by 4% paraformaldehyde (PFA) in PBS. Brains were removed, post-fixed and frozen at −80 °C after cryoprotection. Brain sections were cut using a Leica cryostat and incubated for 1 h at room temperature (RT) with 10% normal goat serum (NGS), 0.3% Triton X-100 in PBS 0.1 M, pH 7.4, then overnight at 4 °C with mouse monoclonal anti-GFAP antibody (Millipore, 1:2500) or rabbit polyclonal anti-Iba1 (Wako Reagent, 1:1000), followed by visualization with the Vectastain ABC kit (Vector), using 3,3′ diaminobenzidine as chromogen. Sections were examined under an Olympus BX61 light microscope. Images were collected at 20× with a camera using AnalySIS software (Soft Imaging Systems version 3.2). Iba1 signals were quantified using ImageJ software (http://rsbweb.nih.gov/ij/) and expressed as area fraction (Perego et al., 2011). Pyramidal neurons in the CA1 region of the hippocampus were counted using ImageJ by an operator (L.P.) blind to the experimental groups. Slices were matched at comparable anteroposterior and dorsoventral levels for comparison of the different experimental groups.

4.5. Statistics

Prism 7.0 (GraphPad Software Inc., San Diego, CA) was used for statistical analyses. Onset and survival times were analyzed by Kaplan-Meier Survival Analysis using the long-rank test to compare the curves. All graphs illustrate the mean ± SEM. For each variable, differences between the groups were assessed using independent one-way analysis of variance (ANOVA) or two-way ANOVA followed by Tukey's *post hoc* analysis (details are reported in the figure legends). *P* values < .05 were considered significant.

Acknowledgments

We thank Elisa R. Zanier for discussion and comments on the manuscript.

Funding

This work was supported by grants from Telethon Italy (TCR08002), the Italian Research Foundation for Amyotrophic Lateral Sclerosis (AriSLA; grant eCypALS), and the Italian Ministry of Health (RF-2013-02356221 and RF-2016-02362950).

References

Aguzzi, A., Zhu, C., 2017. Microglia in prion diseases. J. Clin. Invest. 127, 3230–3239.
Bell, R.D., Winkler, E.A., Singh, I., Sagare, A.P., Deane, R., Wu, Z., Holtzman, D.M., Betsholtz, C., Armulik, A., Sallstrom, J., Berk, B.C., Zlokovic, B.V., 2012. Apolipoprotein E controls cerebrovascular integrity via cyclophilin a. Nature 485, 512–516.
Bertani, I., Iori, V., Trusel, M., Maroso, M., Foray, C., Mantovani, S., Tonini, R., Vezzani, A., Chiesa, R., 2017. Inhibition of IL-1β signaling normalizes NMDA-dependent neurotransmission and reduces seizure susceptibility in a mouse model of Creutzfeldt-Jakob disease. J. Neurosci. 37, 10278–10289.
Bouybayoune, I., Mantovani, S., Del Gallo, F., Bertani, I., Restelli, E., Comerio, L., Tapella, L., Baracchi, F., Fernandez-Borges, N., Mangieri, M., Bisighini, C., Beznoussenko, G.V., Paladini, A., Balducci, C., Micotti, E., Forloni, G., Castilla, J., Fiordaliso, F., Tagliavini, F., Imeri, L., Chiesa, R., 2015. Transgenic fatal familial insomnia mice indicate prion infectivity-independent mechanisms of pathogenesis and phenotypic expression of disease. PLoS Pathog. 11, e1004796.
Carroll, J.A., Chesebro, B., 2019. Neuroinflammation, microglia, and cell-association during prion disease. Viruses 11.
Carroll, J.A., Striebel, J.F., Rangel, A., Woods, T., Phillips, K., Peterson, K.E., Race, B., Chesebro, B., 2016. Prion strain differences in accumulation of PrPSc on neurons and glia are associated with similar expression profiles of neuroinflammatory genes: comparison of three prion strains. PLoS Pathog. 12, e1005551.
Carroll, J.A., Race, B., Williams, K., Striebel, J., Chesebro, B., 2018. Microglia are critical in host defense against prion disease. J. Virol. 92 (15). https://doi.org/10.1128/JVI.00549-18. pii: e00549-18.
Chiesa, R., Piccardo, P., Ghetti, B., Harris, D.A., 1998. Neurological illness in transgenic mice expressing a prion protein with an insertional mutation. Neuron 21, 1339–1351.
Cohen, E., Taraboulos, A., 2003. Scrapie-like prion protein accumulates in aggresomes of cyclosporin A-treated cells. EMBO J. 22, 404–417.
Colby, D.W., Prusiner, S.B., 2011. Prions. Cold Spring Harb. Perspect. Biol. 3, a006833.
Colgan, J., Asmal, M., Neagu, M., Yu, B., Schneidkraut, J., Lee, Y., Sokolskaja, E., Andreotti, A., Luban, J., 2004. Cyclophilin a regulates TCR signal strength in CD4+ T cells via a proline-directed conformational switch in Itk. Immunity 21, 189–201.
Cunningham, C., Wilcockson, D.C., Campion, S., Lunnon, K., Perry, V.H., 2005. Central and systemic endotoxin challenges exacerbate the local inflammatory response and

increase neuronal death during chronic neurodegeneration. J. Neurosci. 25, 9275–9284.
Dawar, F.U., Xiong, Y., Khattak, M.N.K., Li, J., Lin, L., Mei, J., 2017. Potential role of cyclophilin a in regulating cytokine secretion. J. Leukoc. Biol. 102, 989–992.
Falsig, J., Julius, C., Margalith, I., Schwarz, P., Heppner, F.L., Aguzzi, A., 2008. A versatile prion replication assay in organotypic brain slices. Nat. Neurosci. 11, 109–117.
Field, R., Campion, S., Warren, C., Murray, C., Cunningham, C., 2010. Systemic challenge with the TLR3 agonist poly I:C induces amplified IFNalpha/beta and IL-1beta responses in the diseased brain and exacerbates chronic neurodegeneration. Brain Behav. Immun. 24, 996–1007.
Fioriti, L., Dossena, S., Stewart, L.R., Stewart, R.S., Harris, D.A., Forloni, G., Chiesa, R., 2005. Cytosolic prion protein (PrP) is not toxic in N2a cells and primary neurons expressing pathogenic PrP mutations. J. Biol. Chem. 280, 11320–11328.
Hickman, S., Izzy, S., Sen, P., Morsett, L., El Khoury, J., 2018. Microglia in neurodegeneration. Nat. Neurosci. 21, 1359–1369.
Kordek, R., Nerurkar, V.R., Liberski, P.P., Isaacson, S., Yanagihara, R., Gajdusek, D.C., 1996. Heightened expression of tumor necrosis factor alpha, interleukin 1 alpha, and glial fibrillary acidic protein in experimental Creutzfeldt-Jakob disease in mice. Proc. Natl. Acad. Sci. U. S. A. 93, 9754–9758.
Lauranzano, E., Pozzi, S., Pasetto, L., Stucchi, R., Massignan, T., Paolella, K., Mombrini, M., Nardo, G., Lunetta, C., Corbo, M., Mora, G., Bendotti, C., Bonetto, V., 2015. Peptidylprolyl isomerase a governs TARDBP function and assembly in heterogeneous nuclear ribonucleoprotein complexes. Brain 138, 974–991.
Legname, G., Virgilio, T., Bistaffa, E., De Luca, C.M.G., Catania, M., Zago, P., Isopi, E., Campagnani, I., Tagliavini, F., Giaccone, G., Moda, F., 2018. Effects of peptidyl-prolyl isomerase 1 depletion in animal models of prion diseases. Prion 12, 127–137.
Liddelow, S.A., Barres, B.A., 2017. Reactive astrocytes: production, function, and therapeutic potential. Immunity 46, 957–967.
Liddelow, S.A., Guttenplan, K.A., Clarke, L.E., Bennett, F.C., Bohlen, C.J., Schirmer, L., Bennett, M.L., Münch, A.E., Chung, W.-S., Peterson, T.C., Wilton, D.K., Frouin, A., Napier, B.A., Panicker, N., Kumar, M., Buckwalter, M.S., Rowitch, D.H., Dawson, V.L., Dawson, T.M., Stevens, B., Barres, B.A., 2017. Neurotoxic reactive astrocytes are induced by activated microglia. Nature 541, 481–487.
Malesević, M., Kühling, J., Erdmann, F., Balsley, M.A., Bukrinsky, M.I., Constant, S.L., Fischer, G., 2010. A cyclosporin derivative discriminates between extracellular and intracellular cyclophilins. Angew Chem Int Ed Engl 49, 213–215.
Moreno, J.A., Halliday, M., Molloy, C., Radford, H., Verity, N., Axten, J.M., Ortori, C.A., Willis, A.E., Fischer, P.M., Barrett, D.A., Mallucci, G.R., 2013. Oral treatment targeting the unfolded protein response prevents neurodegeneration and clinical disease in prion-infected mice. Sci. Transl. Med. 5, 206ra138.
Pasetto, L., Pozzi, S., Castelnovo, M., Basso, M., Estevez, A.G., Fumagalli, S., De Simoni, M.G., Castellaneta, V., Bigini, P., Restelli, E., Chiesa, R., Trojsi, F., Monsurrò, M.R., Callea, L., Malešević, M., Fischer, G., Freschi, M., Tortarolo, M., Bendotti, C., Bonetto, V., 2017. Targeting extracellular Cyclophilin a reduces Neuroinflammation and extends survival in a mouse model of amyotrophic lateral sclerosis. J. Neurosci. 37, 1413–1427.
Perego, C., Fumagalli, S., De Simoni, M.-G., 2011. Temporal pattern of expression and colocalization of microglia/macrophage phenotype markers following brain ischemic injury in mice. J. Neuroinflammation 8, 174.
Quaglio, E., Restelli, E., Garofoli, A., Dossena, S., De Luigi, A., Tagliavacca, L., Imperiale, D., Migheli, A., Salmona, M., Sitia, R., Forloni, G., Chiesa, R., 2011. Expression of mutant or cytosolic PrP in transgenic mice and cells is not associated with endoplasmic reticulum stress or proteasome dysfunction. PLoS One 6, e19339.
Restelli, E., Fioriti, L., Mantovani, S., Airaghi, S., Forloni, G., Chiesa, R., 2010. Cell type-specific neuroprotective activity of untranslocated prion protein. PLoS One 5, e13725.
Roucou, X., Guo, Q., Zhang, Y., Goodyer, C.G., LeBlanc, A.C., 2003. Cytosolic prion protein is not toxic and protects against Bax-mediated cell death in human primary neurons. J. Biol. Chem. 278, 40877–40881.
Schultz, J., Schwarz, A., Neidhold, S., Burwinkel, M., Riemer, C., Simon, D., Kopf, M., Otto, M., Baier, M., 2004. Role of interleukin-1 in prion disease-associated astrocyte activation. Am. J. Pathol. 165, 671–678.
Sharief, M.K., Green, A., Dick, J.P., Gawler, J., Thompson, E.J., 1999. Heightened intrathecal release of proinflammatory cytokines in Creutzfeldt-Jakob disease. Neurology 52, 1289–1291.
Sikorska, B., Knight, R., Ironside, J.W., Liberski, P.P., 2012. Creutzfeldt-Jakob disease. Adv. Exp. Med. Biol. 724, 76–90.
Syed, F., Rycyzyn, M.A., Westgate, L., Clevenger, C.V., 2003. A novel and functional interaction between cyclophilin a and prolactin receptor. Endocrine 20, 83–90.
Tamguney, G., Giles, K., Glidden, D.V., Lessard, P., Wille, H., Tremblay, P., Groth, D.F., Yehiely, F., Korth, C., Moore, R.C., Tatzelt, J., Rubinstein, E., Boucheix, C., Yang, X., Stanley, P., Lisanti, M.P., Dwek, R.A., Rudd, P.M., Moskovitz, J., Epstein, C.J., Cruz, T.D., Kuziel, W.A., Maeda, N., Sap, J., Ashe, K.H., Carlson, G.A., Tesseur, I., Wyss-Coray, T., Mucke, L., Weisgraber, K.H., Mahley, R.W., Cohen, F.E., Prusiner, S.B., 2008. Genes contributing to prion pathogenesis. J Gen Virol 89, 1777–1788.
Tribouillard-Tanvier, D., Striebel, J.F., Peterson, K.E., Chesebro, B., 2009. Analysis of protein levels of 24 cytokines in scrapie agent-infected brain and glial cell cultures from mice differing in prion protein expression levels. J. Virol. 83, 11244–11253.
Tribouillard-Tanvier, D., Carroll, J.A., Moore, R.A., Striebel, J.F., Chesebro, B., 2012. Role of cyclophilin A from brains of prion-infected mice in stimulation of cytokine release by microglia and astroglia in vitro. J. Biol. Chem. 287, 4628–4639.
Vezzani, A., Viviani, B., 2015. Neuromodulatory properties of inflammatory cytokines and their impact on neuronal excitability. Neuropharmacology 96, 70–82.
Vincenti, J.E., Murphy, L., Grabert, K., McColl, B.W., Cancellotti, E., Freeman, T.C., Manson, J.C., 2015. Defining the microglia response during the time course of chronic neurodegeneration. J. Virol. 90, 3003–3017.
Williams, A., Lucassen, P.J., Ritchie, D., Bruce, M., 1997. PrP deposition, microglial activation, and neuronal apoptosis in murine scrapie. Exp. Neurol. 144, 433–438.
Yurchenko, V., Zybarth, G., O'Connor, M., Dai, W.W., Franchin, G., Hao, T., Guo, H., Hung, H.-C., Toole, B., Gallay, P., Sherry, B., Bukrinsky, M., 2002. Active site residues of cyclophilin A are crucial for its signaling activity via CD147. J. Biol. Chem. 277, 22959–22965.
Zhu, C., Herrmann, U.S., Falsig, J., Abakumova, I., Nuvolone, M., Schwarz, P., Frauenknecht, K., Rushing, E.J., Aguzzi, A., 2016. A neuroprotective role for microglia in prion diseases. J. Exp. Med. 213, 1047–1059.